

ABSTRACT

Title of Thesis: ASSESSING THE IMPACTS OF NON-
POINT SOURCE FRESHWATER AND
NUTRIENT INPUTS ON A SHALLOW
COASTAL ESTUARY

Thomas Wyatt Butler, Master of Science, 2019

Thesis Directed By: Dr. Raleigh Hood, Professor, University of
Maryland Center for Environmental Science

Academic research models for Chesapeake Bay have, traditionally, been forced with USGS inputs, flows and nutrient loads from 10 major rivers. These tributaries fail to account for 100% of the inputs entering the Bay. In contrast, models used for determining Total Maximum Daily Load for Chesapeake Bay are forced with output from a watershed model at thousands of locations, presumably, accounting for all these inputs. Our aim is to increase understanding of the impacts different forcing schemes have on water quality model simulation. Simulations were completed using three forcing approaches: 1) using “traditional” USGS-derived input from 10 major rivers; 2) using “concentrated” input from 10 major rivers derived from watershed model output; and 3) using “diffuse” input from 1117 rivers derived from watershed model output. Comparisons of these schemes revealed large impacts on simulations in Chesapeake Bay during periods of high flow and extreme weather events under diffuse forcing.

ASSESSING THE IMPACTS OF NON-POINT SOURCE FRESHWATER AND
NUTRIENT INPUTS ON A SHALLOW COASTAL ESTUARY

by

Thomas W. Butler

Thesis submitted to the Faculty of the Graduate School of the
University of Maryland, College Park, in partial fulfillment
of the requirements for the degree of
[Master of Science]
[2019]

Advisory Committee:
Professor [Dr. Raleigh Hood], Chair
[Mr. Gary Shenk]
[Dr. Victoria Coles]

© Copyright by
[Thomas W. Butler]
[2019]

Preface

The eutrophication of coastal environments is a large issue and models are a useful tool to study the impacts of nutrient reductions on restoration efforts. But many current models fail to accurately capture the loading of water and nutrients due to limited observational data. Therefore, expanding the ability of existing models to incorporate more realistic input from rivers is essential to increasing the applicability of numerical models to estuarine studies.

Dedication

I would like to dedicate this master thesis my friends and family for the tremendous support I have received throughout the process.

Acknowledgements

I would like to thank:

- Dr. Raleigh Hood
- Dr. Victoria Coles
- Mr. Gary Shenk
- HPL Education Committee
- SESYNC
- Hood Lab
- Chesapeake Bay Program
- Horns Point Community
- My Loving Friends and Family

Table of Contents

Preface.....	i
Dedication.....	ii
Acknowledgements.....	iii
Table of Contents.....	iv
List of Tables.....	v
List of Figures.....	vi
List of Abbreviations.....	viii
Chapter 1: The impacts of non-point source freshwater inputs on a shallow coastal estuary, Chesapeake Bay.....	1
Introduction 1.....	1
Methods 2.....	4
Physical Module 2.1.....	4
Biogeochemical Module 2.2.....	5
Model Forcing Data 2.3.....	6
Coupling Models 2.4.....	8
Parameterization 2.5.....	9
Model Runs 2.6.....	10
Results 3.....	10
Flow Comparison 3.1.....	10
Diffuse vs Traditional Flow 3.1.1.....	10
Diffuse vs Traditional Flow 3.1.2.....	11
Model Validation 3.2.....	11
Traditional Forcing Validation 3.2.1.....	12
Concentrated Forcing Validation 3.2.2.....	12
Diffuse Forcing Validation 3.2.3.....	13
Validation Conclusions 3.2.4.....	14
Difference Results 3.3.....	15
Diffuse Forcing Differences 3.3.1.....	16
Concentrated Forcing Differences 3.3.2.....	18
Hypoxic Volume Differences 3.3.3.....	21
Discussion 4.....	21
Conclusions 5.....	25
Bibliography.....	27

List of Tables

Table 1. Model run scenario descriptions	31
Table 2. Comparison of annual hypoxic volume for difference forcing schemes.	31
Table 3. Comparison of summed annual nitrate load for the entire Chesapeake Bay, 2005	31

List of Figures

- Figure 1.** a) ChesROMS grid domain; b) Bathymetric plot of ChesROMS model with 10 major rivers from a traditional forcing scheme. 32
- Figure 2.** Biogeochemical flows throughout ChesROMS Wiggert et al. (2017) 33
- Figure 3.** Comparison of Concentrated vs Diffuse River Forcing input locations into Chesapeake Bay. 34
- Figure 4.** (a) Comparison of the cumulative sum of river discharge for each forcing scheme over the course of 2005 and (b) a comparative time series of total riverine discharge into Chesapeake Bay for 2005. 35
- Figure 5.** Model skill results from validation of a Traditional forcing scheme plotted spatially for a) Chlorophyll, b) NH₄, c) NO₃, d) Oxygen, e) Salt, f) Temperature. 36
- Figure 6.** Model skill results from validation of a Diffuse forcing scheme plotted spatially for a) Chlorophyll, b) NH₄, c) NO₃, d) Oxygen, e) Salt, f) Temperature. 37
- Figure 7.** Model skill results from validation of a Concentrated forcing scheme plotted spatially for a) Chlorophyll, b) NH₄, c) NO₃, d) Oxygen, e) Salt, f) Temperature. 38
- Figure 8.** Comparison of monthly averaged difference values for NH₄ (a,f), NO₃ (b,g), oxygen (c,h), salinity (d,i) and temperature (e,j) for the diffuse and concentrated forcing cases compared to traditional forcing for each ChesROMS cell along a vertical section over the entire length of the mainstem Chesapeake Bay deep channel. The differences between diffuse and traditional forcing cases are shown in left hand panels and the differences between the concentrated and traditional forcing cases are shown in the right-hand panels. 39
- Figure 9.** Months of largest differences between Diffuse and Traditional Forcing along a vertical section in the deep channel of the mainstem Bay for a) NO₃, b) Oxygen, c) Salinity, d) Temperature and in the bottom layer of ChesROMS for e) NO₃, f) Oxygen, g) Salinity, h) Temperature. 40
- Figure 10.** Months of largest differences between Concentrated and Traditional Forcing along a vertical section in the deep channel of the mainstem Bay for a) NO₃, b) Oxygen, c) Salinity, d) Temperature and in the bottom layer of ChesROMS for e) NO₃, f) Oxygen, g) Salinity, h) Temperature. 41

Figure 11. Averaged monthly hypoxic volume (km³) under different forcing schemes for the year 2005.

42

List of Abbreviations

ChesROMS- Chesapeake Bay Regional Ocean Modelling System	TN- Total Nitrogen
USGS- United States Geological Survey	TP- Total Phosphorus
TMDL- Total Maximum Daily Load	Chla-a- Chlorophyll-a
CBP- Chesapeake Bay Program	BGC- Biogeochemical
WSM- Watershed Model	DO- dissolved oxygen
US EPA- United States Environmental Protection Agency	PO₄ -phosphate
WIP- Watershed Implementation Plan	NH₄ -ammonium
NPZD- nutrients (N), phytoplankton (P), zooplankton (Z) and detritus (D)	NO₃ - nitrate
DON- Dissolved Organic Nitrogen	totN- total nitrogen
CBPWM- Chesapeake Bay Program Watershed Model	totP- total phosphorus
RIMPS- River Input Monitoring Program Station	orgP- organic phosphorus
	orgN- organic nitrogen
	PIP- particulate inorganic phosphorus
	TOC- total organic carbon
	TSS- total suspended solids

Chapter 1: The impacts of non-point source freshwater inputs on a shallow coastal estuary, Chesapeake Bay

Introduction 1

Chesapeake Bay is the largest estuary in North America and has the highest land-to-water ratio (14:1) of any coastal water body in the world US NPS <<https://www.nps.gov/chba/learn/nature/facts-and-formation.htm>> Accessed 09/26/19. This high land to water ratio influences water quality to a greater degree than watersheds with lower land to water ratios. The Chesapeake Bay watershed consists of portions of Delaware, Maryland, New York, Pennsylvania, Virginia, West Virginia, and the District of Columbia (Kemp et al. 2005). Such a large area encompasses approximately 167,000 km² populated by roughly 18 million people (Testa et al. 2017). The land-based activities of these citizens have major impacts upon the water quality in all parts of Chesapeake Bay. On May 12, 2009 President Barack Obama signed Executive Order 13508 (<https://federalleadership.chesapeakebay.net/page/About-the-Executive-Order.aspx>) recognizing Chesapeake Bay as a national treasure and calling upon the federal government to renew efforts to restore and protect the nation's largest estuary and its watershed. Following the executive order, a Total Maximum Daily Load (TMDL) was established for Chesapeake Bay on December 29, 2010 (<https://www.epa.gov/chesapeake-bay-tmdl>). Chesapeake Bay's TMDL represents a comprehensive pollution diet with mandated reductions of pollutants to achieve approved water quality standards U.S. EPA (U.S. Environmental Protection Agency) 2010. Chesapeake Bay Total Maximum Daily Load for Nitrogen, Phosphorus, and Sediment. USEPA, Philadelphia, PA <<http://www.epa.gov/chesapeake-bay-tmdl/chesapeake-bay-tmdl-document>>. Accessed 1/8/2018.

The Chesapeake Bay TMDL Document mandates that the required pollution controls to achieve nutrient reductions be in place by 2025 with a midpoint assessment in 2017. In addition to this midpoint assessment the EPA conducts biennial reviews of each jurisdiction's milestone commitments. If progress is not being met then increased oversight is required and changes must be made to that jurisdiction's watershed implementation plan (WIP). This WIP is designed to reduce pollution within a specific jurisdiction and so is altered accordingly with goals and milestones set by that jurisdiction. Results of the 2017 midpoint assessment indicate the required reductions in Phosphorus and Sediment were met but not those for Nitrogen USEPA, Philadelphia, PA < <https://www.epa.gov/chesapeake-bay-tmdl/epa-final-evaluation-2016-2017-milestone-and-midpoint-progress-and-2018-2019>>. Accessed 7/01/2019. Since reductions in Nitrogen were not met in the 2017 midpoint assessment a new WIP phase 3 was constructed for each jurisdiction. During the initial stages of the TMDL formulation various stakeholders systematically evaluated and agreed on approaches to address multiple technical aspects related to developing the Bay TMDL. One of the agreed upon methods to develop effective strategies for reaching the TMDL was the utilization of numerical models. The Chesapeake Bay Program (CBP) is tasked with formulating the TMDL. The CBP currently runs a suite of coupled models to predict the impacts of management practices on the water quality of the tributaries of Chesapeake Bay (Hood et al. 2019). This modeling suite has been a crucial tool in the implementation of TMDL's across the Chesapeake Bay watershed, as well as the development of these new WIPs.

The CBP water quality and sediment transport model is currently linked to the WSM via 2928 cells (Cercio and Noel 2017). The WSM is currently employed as a management tool to assess the achievement of milestones within each jurisdiction of the Chesapeake Bay watershed (USEPA). The water quality and sediment transport model coupled with the WSM to determine the effects of nutrient reductions across the Chesapeake Bay watershed(USEPA). In comparison, many academic models such as the Chesapeake Bay Regional Ocean Modeling System (ChesROMS) are forced with only 9-10 of the largest rivers in the watershed (Feng et al. 2015; Wiggert, Hood, and Brown 2017).The USGS has been collecting data at the 9 main river input

monitoring program stations (RIMPS) since 1985, knowing these stations account for ~90% of the freshwater entering the Bay. Subsequent work has only reinforced this knowledge (Zhang and Blomquist 2018). As such, the convention of using only these major rivers has been standard practice for multiple academic models (Irby et al. 2016).

Comparing this regulatory model with academic models has proven valuable for assessing uncertainty in model predictions and has helped to create more accurate projections of water quality after the application of management practices (Irby et al. 2016). Increasing the realism of these academic models would be extremely valuable to stakeholders developing TMDL strategies ((Irby et al. 2018; Da, Friedrichs, and St-Laurent 2018)). One such model which has been widely applied in Chesapeake Bay and compared with the CBP models is the Chesapeake Bay Regional Ocean Modelling System (ChesROMS) (Xu et al. 2012; Scully 2016; Feng et al. 2015; Brown et al. 2013; Bever et al. 2013). This model has been run by numerous researchers (e.g., (Testa and Kemp 2014; Scully 2016; Feng et al. 2015; Bever et al. 2013; Wiggert, Hood, and Brown 2017)). Several watershed models such as the Dynamic Land Ecosystem Model (Feng et al. 2015) and the Chesapeake Bay Program Watershed Model have been linked (Irby and Friedrichs 2019) with ChesROMS. These forcing's however still utilize the same 9-10 major rivers as forcing points, although they do add in the remaining flow to these major rivers. It has been shown that the river loads strongly influence the Chesapeake Bay's water quality (Williams et al. 2010). Given that many academic models neglect the full spatial distribution and loading of watershed flow and nutrients into estuarine environments, it is the goal of this research to incorporate the correct loading and spatial patterns of forcing into a numerical model, ChesROMS.

In this paper I take CBWSM output and link this to ChesROMS following similar methods to those used in Testa et al. (2014). Although these linkages allow me to draw spatial relationships between cells they do not accurately capture the full watershed discharge and nutrient concentrations. This new forcing along a diffuse boundary consists of 1117 cells, each consisting of water input which force the model. By linking the WSM to ChesROMS I can capture additional riverine

discharge data which is otherwise omitted. Spatially the resolution of the grid is unchanged but riverine input locations are changed creating new freshwater inputs in each existing cell which are previously not present, such as the Patapsco. I am additionally able to link a regulatory framework to academic models with a spatial resolution accounting for many small tributaries. This increased spatial resolution combined with the linkage to a model with a regulatory component increase the accuracy and realism of model results.

Methods 2

Physical Module 2.1

The physical component of the coupled model is based on the Regional Ocean Modeling System (ROMS) (Shchepetkin and McWilliams 2005) version 3.6. The model domain and horizontal grid follow the Chesapeake Bay community implementation of ROMS (ChesROMS) (Xu et al. 2012). The domain spans the region from 77.2°W to 75.0°W and from 36°N to 40°N, covering the main stem and primary tributaries of the Chesapeake Bay, as well as part of the mid-Atlantic Bight (Fig. 1a). The horizontal grid spacing varies with the smallest grid size (430 m/cell) in the northern Bay near the Chesapeake and Delaware Canal, with the largest grid sizes (10 km/cell) in the southern end of the mid-Atlantic Bight, and average grid spacing within the Chesapeake Bay of 1.7 km. This resolution is not to be confused with the model's predictive ability which is best in the mainstem deep channel of the Bay. In these areas the model's spatial resolution is lower. The model has 20 terrain-following vertical layers with higher resolution near the surface and bottom boundaries. The bottom topography is also smoothed to avoid pressure gradient errors caused by steep bathymetry (Xu et al. 2012). The TSMPDATA advection scheme is used in this study following (Feng et al. 2015).

ChesROMS is forced by open ocean tides and non-tidal water level, river discharge, winds, and heat exchange across the air–water interface. Water level forcing at the oceanic boundary includes nine tidal harmonic constituents and the observed non-tidal water level based on an interpolation between observed values at

Duck, NC and Wachapreague, VA. Chapman's condition for surface elevation and Flather's condition for barotropic velocity is applied to the barotropic component at the open ocean boundary. For the baroclinic component a radiation condition is used for velocity and a radiation condition with nudging is used for temperature and salinity. Climatological temperature and salinity from the World Ocean Atlas 2001 were used for nudging at the open ocean boundary. For additional details on how the physical model is configured and forced see (Xu et al. 2012).

Biogeochemical Module 2.2

The biogeochemical model is based on an NPZD-type, nitrogen-based ecosystem model (Fennel et al. 2006). The model has been modified as described in (Wiggert, Hood, and Brown 2017) (Fig. 2) and it is very similar to the model described in Feng et al. (2015). Here I focus on the components of the model that differ from (Feng et al. 2015). The detailed model equations and parameters are presented in Wang (in preparation). The biogeochemical model contains ten state variables: phytoplankton, chlorophyll, zooplankton, ammonium, nitrate, dissolved organic nitrogen, inorganic suspended sediment, small detritus, large detritus and oxygen. Except for chlorophyll, oxygen and ISS, all the state variables are in nitrogen units.

The original (Fennel et al. 2006) biogeochemical model assumes aerobic respiration in the water column and a fixed fraction (14%) of anoxic remineralization in the sediments. However, during the summertime in Chesapeake Bay the sub-pycnocline water column transitions to hypoxic and fully anoxic conditions in the mesohaline deep channel and, as a result, the sediments also transition to fully anoxic conditions (Kemp et al. 2009; Kemp et al. 2005). In order to account for the impacts of changing water column oxygen concentrations our model has been modified as described in (Wiggert, Hood, and Brown 2017) to allow the ratio of anaerobic to aerobic remineralization to change in response to changes in the oxygen concentrations in the overlying water column extending all the way to a fully anoxic overlying water column with the bottom sediment transitioning to fully anaerobic remineralization.

The dissolved organic nitrogen (DON) pool is of a similar magnitude to the inorganic nitrogen pool in Chesapeake Bay (Boynton et al. 1995) and it has a pronounced effect on the nitrogen budget in the estuary (Bradley et al. 2010). Therefore, a single DON state variable was added to the model as described in (Wiggert, Hood, and Brown 2017). The sources of DON are from the river, algal exudation and mortality, and zooplankton excretion. This DON is remineralized both aerobically and anaerobically like particulate organic nitrogen throughout the year. In addition, following the (Fasham, Ducklow, and McKelvie 1990) I assume that a fraction of the zooplankton excretion is in the form of ammonium and rest is in the form of DON. This transfer of a substantial fraction of zooplankton excretion into the DON pool was not included in the previous versions of the model (Feng et al. 2015; Wiggert, Hood, and Brown 2017).

The light attenuation model is the same as that which is described in (Xu, Hood, and Chao 2005). Following (Xu and Hood 2006), the sinking speed for phytoplankton varies as a function of season with a high sinking speed in winter and spring to represent the dominance of large diatoms that sink rapidly, while during summer, the sinking speed is reduced to represent the dominance of small flagellates and dinoflagellates that sink slowly. Here the changes in sinking speed are modulated as a continuous function of temperature; this contrasts with the step function changes used in (Xu and Hood 2006).

Model Forcing Data 2.3

The data used to force ChesROMS were obtained from the Chesapeake Bay Program Watershed Model as well as the North American Regional Reanalysis (NARR) database. NARR data provided wind and climate forcing at a three-hour timestep for the year 2005 while riverine inputs were obtained either from USGS data or the CBP watershed model (CBPWM).

The traditional methods that have been used to force ChesROMS have used observational river data. The observational data (Testa et al. 2014; Irby et al. 2016) is managed by the United States Geological Survey (USGS) as part of the River Input Monitoring Program (RIMP) and provides information regarding river discharge as

well as water quality variables that include total nitrogen (TN) total phosphorus (TP), and chlorophyll a (chl-a) to name a few (Williams 2010). This method of forcing ChesROMS relies on data from 9 or 10 major Chesapeake Bay tributaries ((Wiggert, Hood, and Brown 2017), Wang in preparation). These include the Nanticoke, Chester, Susquehanna, Patuxent, Potomac, Rappahannock, York, and James River, as well as a river representing the Delaware Canal (Fig.1). For my application of the model there is no correction factor for missed flow from due to the omission of smaller freshwater inputs. Daily USGS inputs for freshwater are utilized for freshwater inputs while monthly average nutrient concentrations are provided. These monthly average concentrations are used to create an interpolation of nutrient concentrations at each day over the course of the year.

The inputs required by the ROMS Biogeochemical module (BGC) do not correspond exactly to the outputs of the hydrological model. Thus, several variables from the CBP watershed model had to be converted to run ChesROMS. The CBP watershed model provides the following: dissolved oxygen, temperature, chlorophyll, flow rate, phosphate (PO_4), ammonium (NH_4), nitrate (NO_3), total nitrogen (totN), total phosphorus (totP), organic phosphorus (orgP), organic nitrogen (orgN), particulate inorganic phosphorus (PIP), total organic carbon (TOC), total suspended solids (TSS), sand, silt, clay, and phytoplankton.

The ChesROMS BGC module is a nitrogen-based model. Therefore, only the physical and nitrogen outputs from the CBP watershed model are needed to force it. Specifically, the BGC module requires the following forcing variables: river flow, temperature, salt, inorganic suspended solids (ISS), small detritus, large detritus, zooplankton, NO_3 , NH_4 , oxygen, phytoplankton, chlorophyll, and dissolved organic nitrogen (DON). The process for converting these variables was such that if the CBP watershed model had a directly comparable variable then it was used directly to force ChesROMS. This was the case for temperature, dissolved oxygen, NH_4 , and NO_3 . For other model state variables, it was necessary to adapt the CBWM forcing. This was the case for the ChesROMS state variables phytoplankton, zooplankton, large detritus, small detritus, and DON.

It was assumed that the CBPWM phytoplankton variable, which has units of mass (mg/l), was approximately 8% nitrogen by weight. Zooplankton concentrations were estimated assuming that zooplankton biomass is 10% of the phytoplankton biomass (Pauly and Christensen 1995). Large and small detritus were estimated by subtracting the phytoplankton nitrogen from total organic nitrogen and then assuming that 70% was large detritus and 30% was small detritus (Van Valkenburg, Jones, and Heinle 1978). The dissolved organic nitrogen was assumed to be the remainder of the organic nitrogen that was not attributed to phytoplankton. In order to calculate the inorganic suspended solid load for ChesROMS the CBWM outputs of sand, silt, clay, and particulate, inorganic phosphorus were all combined. Finally, the river input salinities were all set to zero as the riverine inputs were all freshwater.

Once all the variables were separated into appropriate ChesROMS variables they were converted into units required by ChesROMS. The year 2005 was selected for this experiment because it represents an average year in term of freshwater flow (Irby et al. 2016) and because USGS data and WSM data were available for this year making it possible to directly compare the impacts of different forcing methods on model results.

Coupling Models 2.4

The CBP watershed model provides river forcing inputs for the CBP estuarine models at 2928 cells which act as rivers (Cerco and Noel 2017). In contrast, the ChesROMS model, which has a much lower resolution, and only requires river forcing 1117 cells. In order to adapt the CBP watershed model output to force ChesROMS it was first necessary to determine where both model grids corresponded spatially. This was done by plotting both model domains within MATLAB. Doing this it was possible to determine the closest cell locations within ChesROMS grid and the CBP estuarine model using a closest point search within MATLAB. Model cells were then linked via forcing documents between the output watershed model cells which corresponded with a freshwater input location within the model. If multiple cells discharged into a single ChesROMS cell these were summed to create a single river. All WSM cells were given a weight whereby a specific freshwater input

location was divided between the cells of the ChesROMS grid. Thus, if one cell from the WSM discharged into several ChesROMS cells this WSM cell was given an equal weight into each ChesROMS cell. ArcGIS 10.4 software and MATLAB were both used to visually inspect the newly created relationships assuring cells were correctly correlated. Once this mapping was completed it was possible to determine how many cells from CBP estuarine model grid fit within each ChesROMS cell. This process was applied to three output files provided by the CBP watershed model that specify surface runoff, river flows, and point source inputs along the entire boundary of Chesapeake Bay.

It should be noted that in the ChesROMS grid the upper Potomac River is “wrapped” northward to minimize the number of grid cells in the model for computational efficiency (Fig. 3). In contrast, the CBP models provide a much more realistic representation of the upper Potomac River. Therefore, the CBP estuarine model grid had to be projected on to the ChesROMS grid in the upper Potomac. This was done using the “lasso capture” tool in MATLAB followed by manual correction.

Parameterization 2.5

Parameter tuning was focused on maximizing skill for chlorophyll, NH_4 , NO_3 , and oxygen with emphasis on the latter. The emphasis on oxygen stems from a desire to assess how changes in the river forcing can impact the attainment of TMDL goals. This application is well suited to multiple models and can provide potential insights into different applications across varied geographic areas. In order to accurately compare the differences attributable only to changes in forcing the model was tuned only once. This tuning was performed based on the traditional forcing scheme with subsequent runs using the same parameter set. Variables which were important to get a strong validation for are thus linked to the occurrence of hypoxia. These variables are oxygen, salinity, and temperature, NO_3 , and NH_4 (Fig. 5).

Model validation followed (Warner, Geyer, and Lerczak 2005; Willmott et al. 1985) whereby Root Mean Square (RMS) was calculated as a metric of finding the magnitude of values surrounding the arithmetic mean of a data series. Validation was conducted by comparing model results and observational data collected from the CBP

monitoring stations. A Model Skill (MS) is then calculated comparing the RMS of modelled results and observations. The range of MS goes from 0 to 1 with 1 being a perfect fit between model and data compared to 0 being unrelated in any way (Willmott et al. 1985).

Model Runs 2.6

Three model runs were carried out and compared (Table 1.). One of the runs used USGS RIMP stations forcing at 10 major rivers, several of which were split due to cell placement bringing the total number of ports to 15 locations. This is the “traditional” forcing method. Another model run used the same 10 rivers input as 15 ports except that river transport was derived from the cells immediately adjacent to the “traditional rivers in the CBP watershed model. This is referred to as the “concentrated” forcing method. Finally, a third model run used all the output from the CBP watershed model forcing, i.e., the main 10 major rivers, input at 15 locations, plus an additional 1102 minor freshwater input locations. This run is referred to as the “diffuse” run. Difference plots were then constructed to demonstrate the impacts of using these different forcing methods.

Results 3

Flow Comparison 3.1

Diffuse vs Traditional Flow 3.1.1

The differences between model river forcing schemes (Table 1) were examined prior to carrying out the model runs (Fig. 4a). Fig. 4 shows that the trends in the three river forcing schemes are similar for 2005. However, there are differences in the amount of discharge, particularly in the early portion of the year. The comparison between the diffuse and traditional forcing reveals that largest flow differences are from day one to day 16. During this period, traditional forcing has anywhere from over 26% more flow than diffuse forcing with several peaks above 40%. From day 16 to day 40 this difference is reduced to 6% more flow for traditional forcing versus

diffuse forcing. After day 40 the difference declines until day 87 when there is below a 1% difference between the forcing schemes. After day 87 traditional forcing provides 6.6% more flow than diffuse forcing. This difference declines continuously with the flow from diffuse forcing surpassing traditional forcing flow at day 192. From day 192 until day 283 the difference between diffuse and traditional forcing grows from a 0% to 4.1% with diffuse forcing having the larger flow. At day 283 there is a pulse of discharge further increasing the difference between diffuse and concentrated forcing from 4.1% to 8.35%. The largest difference occurs at the end of 2005 when annual sum of diffuse forcing is 12.7% larger compared to traditional forcing.

Diffuse vs Traditional Flow 3.1.2

The concentrated forcing scheme has a similar discharge pattern compared to the traditional forcing, but the flows are always smaller. From days 1 to 16 there is a significantly larger riverine discharge from traditional forcing with over 99% more flow until day 2. After day 2 this difference shrinks to 52.9% by day 6. From day 6 to day 16 there are fluctuations between 55.5% and 43.9% more flow for traditional forcing. From day 16 to day 40 there is a sharp drop in the difference between traditional and concentrated forcing to 24% more flow for traditional forcing. The difference in flow continues to decrease until day 80 at which time there is only 20% more flow for traditional forcing. From day 80 to day 95 there is another increase in percent difference with traditional forcing having 25.4% more flow compared to concentrated forcing. Between day 95 and day 101 this difference shrinks abruptly to 22% more flow under traditional forcing. This percent difference shrinks from 22% to 21.3% by day 192 and then hovers around 20% until day 283. From day 296 onward this difference declines to, ultimately, 11.5% by the years' end with the traditional forcing having a higher discharge compared to concentrated forcing.

Model Validation 3.2

Model tuning and validation was focused on temperature, salinity, NO_3 , NH_4 and oxygen (Fig. 5). Annual average spatial model skill results for diffuse, concentrated,

and traditional forcing runs are shown using approximately 100 CBP monitoring stations throughout the Bay (Figs. 4,5,6).

Traditional Forcing Validation 3.2.1

With the traditional forcing the model skill for chlorophyll is generally below 0.5 with the worst performance occurring in the tributaries and shallow flanks of the mainstem Bay and the best occurring in the deep channel. For NH_4 model skill is below 0.3 in several tributaries as well as stations near the mouth of the Bay. Approaching the deep channel of the Bay model skill improves to over 0.4 with skill greater than 0.6 for the middle upper Bay. Model skill for NO_3 is the also lowest in the tributaries and on the flanks of the mainstem Bay 0.3 and 0.5. Again, the skill improves in the deep channel middle upper Bay to > 0.8 . Oxygen skill is > 0.6 everywhere with the lowest values found in several tributaries, specifically in the Susquehanna, Patapsco, and Patuxent Rivers. Model skill for oxygen is > 0.8 over the rest of the Bay. Salinity model skill is noticeably lower at the head of several tributaries such as the Susquehanna and Potomac rivers with scores below 0.1 are observed. In tributaries such as the Rappahannock and York rivers model skill at the river head is roughly 0.4-0.5 but increases to above 0.7 near the river mouths. The skill scores for salinity are highest in the deep channel with values all between 0.6 and 0.9. Temperature model skill is above 0.9 at all locations throughout the Bay.

Concentrated Forcing Validation 3.2.2

With the concentrated forcing chlorophyll skill scores are 0.3 or below for the upper Bay and these low scores are also present in the upper Potomac and Choptank Rivers. Model skills scores improve going downriver and are all above 0.3 in the deep channel of the Bay with higher scores (~ 0.5) in the lower mainstem Bay. Skill score values for NH_4 are 0.3 near the mouths of the Susquehanna and Choptank Rivers, and at the head of the York river, and the NH_4 skill scores are just above 0.3 near the mouth of the Bay. The scores increase along the flanks of the mainstem Bay to around 0.5 with NH_4 skill scores nearing 0.6 for the deep channel of the middle Bay. Scores are slightly lower (~ 0.55) for the lower Bay deep channel. Model scores for

NO₃ are lowest in the tributaries of the lower Bay such as the head of the Potomac, Nanticoke, and Rappahannock Rivers, each with a score around 0.45. NO₃ skill scores in the upper and lower mainstem Bay NO₃ are roughly 0.65 while the middle Bay deep channel they are above 0.8. Model skill for oxygen is above 0.6 for the entire bay with scores around 0.65 in the head of the Potomac and Patapsco Rivers, one upper mainstem Bay station and at the mouth of the Choptank River. Over the rest of the Bay model skill for oxygen is 0.8 or higher. Salinity model skills are lower at the head of the Potomac and Susquehanna Rivers with values near 0 but the scores rapidly increase to 0.6 and 0.5 down Bay. Skill scores increases in the deep channel nearing 0.8 with slightly higher scores along the western shore (0.75) compared to the eastern shore (0.6). Model skill for temperature is uniform across the entire Bay with values above 0.9.

Diffuse Forcing Validation 3.2.3

With diffuse forcing chlorophyll model skill is low in several regions with the lowest score at the mouth of the Susquehanna river near 0. The upper and middle Bay skill scores do not exceed 0.4, although scores improve from below 0.3 in the upper mainstem Bay to almost 0.4 in the middle mainstem Bay. The highest model skills are recorded in the deep channel of the lower Bay where model skill for chlorophyll reaches 0.6. Skill scores for NH₄ are low score at the head of the Bay (~0.1) with skill increasing in the middle mainstem Bay to between 0.4 and up to 0.9 in the deep channel. NH₄ skill scores in the Tributaries along the eastern shore in the middle Bay are relatively low (~0.3). Skill in the Patuxent, Rappahannock, and York Rivers is consistently below 0.3 while the Potomac, York, and Nanticoke rivers have skills around 0.5. NH₄ skill scores in the lower mainstem Bay are between 0.5 and 0.6 decreasing to 0.2 at the Bay's mouth. NO₃ skill is lowest in the Rappahannock where values range from 0.2 to 0.35. The head of the York River has a very low score near 0 but quickly improves to 0.65 in the middle of the River. Portions of the middle Patuxent River are also around 0.3 with a higher score of 0.65 at the River's head and 0.9 at the River's mouth. NO₃ skill scores in the lower Bay eastern shore are generally around 0.4 with deep channel scores rising to 0.8. The middle mainstem

Bay has the highest model scores exceeding 0.9 in the deep channel. Upper Bay scores are generally lower but still around 0.65. Oxygen model skill is generally high across the Bay with the lowest scores (~ 0.65) at the head of the Potomac River, mouth of the Choptank River, and one station near the Delaware Canal. The rest of the Bay has skill scores above 0.8. Salinity skill is the lowest (near 0) in the head of the Bay near the Susquehanna River and at the head of the Potomac River. The Rappahannock, York, and James Rivers all have salinity skills between 0.3 and 0.5. Further up the Bay the Patuxent and Nanticoke rivers have skill scores of 0.6. The skill scores in the lower mainstem Bay stations are ~ 0.8 while the middle Bay stations have a scores closer to 0.9. Temperature skill across the Bay does not vary and is in excess of 0.9 at all stations.

Validation Conclusions 3.2.4

Validation results demonstrate that ChesROMS simulations for temperature and oxygen throughout the entire Bay regardless of the type of river forcing employed show high agreement with observational data. Salinity, NO_3 , and NH_4 all show high agreement between observations and model results within the deep channel of the Bay under all tested forcing schemes. The highest agreement is in the upper middle Bay with lower model skill moving towards the lower Bay. Skill results are the lowest in the Bay's tributaries with the lowest scores being seen near the Patuxent, Rappahannock, York, and Nanticoke Rivers. Chlorophyll skill is the lowest of all parameters and shows greater skill in the lower Bay deep channel and lower results in the shallow flanks and upper Bay.

These validation results show that, for chlorophyll, traditional forcing gives the highest model skill followed by concentrated and then diffuse forcing, although the differences are very slight. In all three forcing cases the same patterns emerge whereby the model more accurately predicts chlorophyll near the deep channel and less accurately predicts chlorophyll in the tributaries. Model simulated NH_4 also has the highest skill under the traditional forcing scheme with lower skills for concentrated and diffuse forcing, again by a small margin. Here also the spatial patterns in skill are similar for all three forcing cases with better agreement with

observations in the mainstem Bay and worse agreement in the tributaries. In contrast to chlorophyll and NH_4 , NO_3 model skill is slightly lower under traditional forcing compared to concentrated which in turn has lower skill than diffuse forcing. Again, the same spatial patterns are observed in all three forcing cases with lower model skill in the tributaries compared to the mainstem Bay. However, it should be noted that for the diffuse forcing case model skill in the lower Bay's tributaries is lower than in the other forcing cases whereas the model skill in mainstem is slightly higher compared to the other cases. Model skill for oxygen is almost identical for all three forcing schemes with the only noticeable difference being found in the Susquehanna and Potomac Rivers. There are, however, slight improvements in the oxygen skill in the upper Bay near the Susquehanna River for concentrated and diffuse forcing and there are slight declines in oxygen skill at the head of the Potomac with traditional forcing. Salinity skill patterns appear similar with traditional and diffuse forcing apart from slightly higher skill in the lower Bay's eastern portion under diffuse forcing. Concentrated forcing has lower salinity model skill throughout the mainstem Bay compared to traditional or diffuse forcing. Model skill is higher for salinity in the mainstem compared to the tributaries for both traditional and diffuse forcing whereas concentrated forcing has higher model skill in several tributaries compared to the mainstem. Model skill for temperature across the Bay under all forcing schemes is above 0.9 indicating the model's strong agreement with predicted and observed temperatures .

Difference Results 3.3

Figure 8 shows histograms of the monthly averaged differences for NH_4 , NO_3 , oxygen, salinity and temperature for the diffuse and concentrated forcing cases compared to traditional forcing. These differences are calculated for each cell along a vertical transect running the length of Chesapeake Bay. Due to the highest model skill in the deep channel this area was selected for the vertical transect. As the differences caused by each forcing scheme were the objective absolute differences were calculated.

Diffuse Forcing Differences 3.3.1

Histograms of differences in NH_4 between the diffuse and traditional forcing cases reveal a similar left skewed distribution with generally elevated NH_4 with diffuse forcing (Figure 8a). Many of the differences are clustered between $\pm 2 \text{ mM/m}^3$ NH_4 for traditional forcing compared with diffuse forcing. Most of these data points are centered around a difference very close to zero. The average difference is a 0.32 mM/m^3 increase in concentration under diffuse forcing. There are several data points reveal that diffuse forcing has up to 4 mM/m^3 more NH_4 than traditional forcing. The spatial patterns in the NH_4 differences between the diffuse and traditional forcing are the largest in the upper Bay but due to the lesser magnitude of the differences are not shown.

The monthly difference histogram for NO_3 (Figure 8b) indicates that diffuse forcing case generally has more NO_3 throughout the year with the average difference being around 18 mM/m^3 . Several locations have large NO_3 differences ($> 60 \text{ mM/m}^3$) although differences greater than 20 mM/m^3 are rare. Mean NO_3 concentrations are 5.25 mM/m^3 higher under diffuse forcing. Some of the largest NO_3 differences occur in April (Figure 9a) when the diffuse forcing case has over 30 mM/m^3 more NO_3 than traditional forcing. This difference occurs primarily in the upper Bay over the entire water column as well as in the surface waters moving down Bay. This same pattern can be seen covering a larger area by water with differences exceeding 10 mM/m^3 into the middle of Chesapeake Bay. Over the remainder of Chesapeake Bay NO_3 concentrations are elevated in the diffuse forcing case by as much as 10 mM/m^3 compared to traditional forcing. Horizontally the bottom layer of the Bay shows this increased NO_3 in the diffuse forcing case primarily in the upper Bay with large differences occurring near the Patapsco River (Figure 9b).

Histograms of the differences in oxygen monthly averages indicate there is generally more oxygen with diffuse forcing although these differences are generally less than 20 mM/m^3 (Figure 8c). The largest oxygen differences between the two runs are on the order of $\pm 40 \text{ mM/m}^3$. On average there is a 0.59 mM/m^3 increase in dissolved oxygen concentrations under diffuse forcing. This result is shown spatially

in Figure 9c, which reveals that a very small portion of the water column in the upper mainstem Bay has 30mM/m^3 less oxygen under diffuse forcing during May.

However, over the rest of the upper Bay oxygen is elevated by $\sim 30\text{mM/m}^3$ in the diffuse forcing case compared to the traditional forcing case. Further down Bay this difference in oxygen content is reduced to $\sim 10\text{mM/m}^3$. Looking horizontally the bottom layer reveals these same trends with some small regions near the head of the Bay having lower oxygen concentrations followed by higher oxygen further down Bay for diffuse forcing case (Figure 9d). Note that the Potomac river also exhibits reduced oxygen content in some areas with diffuse forcing compared to traditional forcing.

Salinity shows a bimodal distribution with a larger peak near zero and a smaller peak at 1.5 PSU (Figure 8d). This result shows that there is a large variability in the salinity difference between diffuse and traditional forcing schemes. Many of these differences reveal a significantly fresher Bay under diffuse forcing by more than 1 PSU. On average there is a -0.27 PSU difference whereby the salinity in Chesapeake Bay decreases under diffuse forcing. The largest salinity differences occur in December (Figure 9e) when virtually the entire Bay is fresher with diffuse forcing compared to concentrated forcing. The spatial extent of the salinity difference over 1 PSU includes portions of the upper Bay, as well as the entire middle and lower Bay. The largest differences are in the middle Bay bottom water where the salinity difference increases to 1.5 PSU saltier water for traditional forcing compared to diffuse forcing. Looking spatially across the bottom horizontal layer of the model's domain (Figure 9f) the largest differences are found in the middle and upper Bay. Significant changes are also apparent in the lower reaches of all the tributaries south of 39.5° N. The smallest differences in salinity are found in the lower mainstem Bay (Figure 9f).

Figure 8e shows that the temperature differences between diffuse and traditional forcing cases are centered around zero with a left skewed tail. This shows that most of the differences between diffuse and traditional forcing are less than 0.5° C although there are several locations where temperature differences exceed 1° C. Thus, with the diffuse forcing the water can be as much as 1°C cooler compared traditional forcing.

The mean temperature difference is a 0.02°C increase in temperature under diffuse forcing. An example of this extreme case is shown in Figure 9g, which plots a section of the monthly average temperature difference between the diffuse and traditional forcing for the month of October, which was the month that had the largest differences. The temperature differences in this time period occur primarily in the bottom water of the Bay with the largest difference occurring in the deep channel of the middle upper mainstem Bay. Looking horizontally at the bottom layer of the Bay during October (Figure 9h) these differences are restricted primarily to the middle upper mainstem of the Bay and that these differences are found on the flanks as well as in the deep channel. The temperature differences in the lower reaches of the Bay's tributaries tend to be the opposite with waters up to 0.4°C cooler for diffuse forcing compared to traditional forcing.

Concentrated Forcing Differences 3.3.2

The mean monthly histogram for NH_4 difference between concentrated and traditional forcing reveals that NH_4 is generally higher with the traditional forcing but there are also many instances where NH_4 is lower by more than $1\text{mM}/\text{m}^3$ in the concentrated forcing run (Figure 8f). On average the concentration is $0.28\text{mM}/\text{m}^3$ lower under concentrated forcing. The overall range of differences between concentrated and traditional forcing's, -4 to $3\text{mM}/\text{m}^3$, is smaller than the differences found between diffuse and traditional forcing. The spatial patterns in the NH_4 differences between the diffuse and traditional forcing are the largest in the upper Bay but due to the lesser magnitude of the differences are not shown.

The mean monthly histogram for NO_3 difference between concentrated and traditional forcing reveals a very similar pattern to diffuse forcing difference, although with a smaller range of values (Figure 8g). Most of NO_3 differences between concentrated and traditional forcing are very small, close to $0\text{mM}/\text{m}^3$ (Figure 8g). The mean difference in concentration is a $2.08\text{mM}/\text{m}^3$ increase under concentrated forcing. In general, the run with concentrated forcing has higher NO_3 than traditional forcing as revealed by the large tail to the left in Figure 8g, with many difference values up to $10\text{mM}/\text{m}^3$. The largest NO_3 differences occur in November (Figure 10a)

when some portions of the upper and middle Bay have more than 30mM/m^3 more NO_3 with concentrated forcing. This positive difference declines with depth and distance down Bay. Bottom waters south of 39°N and surface waters south of 38.2°N all show less than 10mM/m^3 increase in NO_3 with concentrated forcing compared to traditional forcing. The horizontal plot for November (Figure 10b) reveals that the largest NO_3 differences along the bottom occur in portions of the upper and middle Bay's western shore as well as in the upper reaches of the Potomac river. There are also large NO_3 differences near the head of the Bay where they transition, moving southward, from 30mM/m^3 more NO_3 to 30mM/m^3 less NO_3 with concentrated forcing compared to traditional forcing.

The mean monthly histogram for oxygen difference between concentrated and traditional forcing reveals that oxygen is generally higher with concentrated forcing (Fig. 8h) with many of the differences being between 0 and 20mM/m^3 . There are also more extreme positive differences reaching 60mM/m^3 compared to 40mM/m^3 for negative differences. Average difference for oxygen concentration is however 0.32mM/m^3 higher under concentrated forcing when compared to traditional forcing. The largest oxygen differences occur during the month of September (Figure 10c) when virtually the entire Bay experiences increased oxygen content under concentrated forcing relative to traditional forcing. The head of the Bay has in excess of 30mM/m^3 more O_2 under concentrated vs traditional forcing. Moving southward there is a small region between 39°N and 39.5°N where the oxygen differences are small which then transitions to a large region throughout the mainstem of the middle Bay where the concentrated forcing run has upwards of 20mM/m^3 more O_2 compared to traditional forcing run. The surface waters over virtually the entire middle and lower Bay exhibit approximately 10mM/m^3 higher oxygen with concentrated forcing. The horizontal plot for September shows that the elevated oxygen values at the bottom with the concentrated forcing are restricted, primarily, to the deep channel (Figure 10f). A large exception to this occurs in the upper Bay where model output reveals significantly higher dissolved oxygen under a concentrated forcing scheme.

Mean monthly average histogram for temperature shows a normal distribution indicating most of the difference between concentrated and traditional forcing are

between +/- 0.5 C. Within this range most of differences are very close to zero (Figure 8j). However, there are several occurrences of warmer water, by up to 1° C, and several occurrences of cooler water, by up to -1° C, with concentrated forcing (Fig. 8j). On average the Bay is 0.02 ° C warmer under concentrated forcing when compared to traditional forcing. The largest temperature differences occur in the month of November (Figure 10g) when a portion of the far upper Bay has over 0.5° C cooler throughout the water column, and a portion off the middle upper Bay deep channel was over 0.5° C warmer with concentrated forcing. Moving down Bay in the deep channel this difference fades to 0.2° C while encompassing the entire water column of the middle Bay. The horizontal view (Figure 10h) shows this same pattern while also revealing considerable spatial variability in the temperature difference between concentrated and traditional forcing runs. The plot also shows the 0.2° C cooler water in the lower portion of the mainstem upper and middle Bay, in addition to the lower reaches of the Patapsco, Rappahannock, and York Rivers are cooler, up to 0.5° C, under concentrated forcing. with concentrated forcing.

The mean monthly histogram for salinity difference between concentrated and traditional forcing reveals a bimodal distribution with peaks ranging around +/- 0.5 PSU. These data suggest the Bay is likely to either be 0.5 PSU fresher or saltier with water being more frequently saltier with concentrated forcing (Fig. 8i). The mean of these values shows a saltier Bay by 0.32 PSU under a concentrated scheme. The most extreme differences approach a +/- 2 PSU, again dominated by waters being saltier. These salinity differences occur in the month of April (Figure 10e) when most of the surface waters of the Bay are over 1.5 PSU saltier with concentrated forcing. Below 5 m depth most of the middle and lower Bay is saltier by 0.75 PSU. The horizontal bottom plot for April shows that the entire bottom the Bay is between 0.5 and 1.5 PSU saltier with concentrated forcing compared to traditional forcing (Figure 10g). The difference in salinity is smaller in the deep channel of the mainstem Bay, 0.5 PSU, compared to the flanks and tributaries where the difference rises to over 1.5 PSU. One anomaly is revealed in the horizontal plot: in the Nanticoke river the salinity is lower by nearly 1 PSU with concentrated forcing compared to traditional forcing.

Hypoxic Volume Differences 3.3.3

The total summed hypoxic volume for the entire year for each forcing case is shown in Table 2. These results show that diffuse forcing has the highest hypoxic volume ($\sim 265 \text{ km}^3$), followed by traditional forcing ($\sim 204 \text{ km}^3$) and finally concentrated forcing ($\sim 110 \text{ km}^3$).

The temporal differences in mean monthly hypoxic volume for each forcing case are plotted in Figure 11. No hypoxia is observed from January to May. The development of hypoxia is first observed in June with the diffuse forcing having the highest average hypoxic volume (0.02781 km^3), followed by traditional forcing (0.00008 km^3), whereas in the concentrated forcing case there is no hypoxia in June. July follows the same trend except with diffuse, traditional, and concentrated forcing having elevated hypoxic volumes of 1.517 , 1.2341 , and 0.3142 km^3 , respectively. The highest monthly average hypoxic volumes are found during August where, again, diffuse forcing has the highest hypoxic volume (5.875 km^3), followed by traditional (4.8086 km^3), followed by concentrated forcing (3.0184 km^3). In September the hypoxic volumes decline following the same trend with diffuse, traditional, and concentrated forcing having elevated hypoxic volumes of 1.102 , 0.7752 , and 0.3519 km^3 , respectively. After September only the diffuse forcing scheme results in a finite hypoxic volume with 0.1653 km^3 in October, and 0.1466 km^3 in November.

Discussion 4

Several different academic models have been applied to Chesapeake Bay to address a wide range of questions and these include applications that help to inform management actions (add citations). Many of these models are forced with USGS data from 10 – 15 rivers that represent the major Chesapeake Bay tributaries. In contrast, the estuarine model that is run by the Chesapeake Bay program for setting Total Maximum Daily Loads (TMDLs) is forced with output from a watershed model that provides inputs from, literally, thousands of rivers. This work demonstrates that there are significant spatial and temporal differences in the model results when an estuarine model is forced with 10 – 15 major rivers versus thousands of rivers.

Specifically, in this study, I measured the differences in ChesROMS model solutions when the model with output from the CBP's watershed model at 1117 locations (diffuse forcing) versus forcing the model in a more traditional manner with USGS data representing only the 10 major rivers (traditional forcing). In addition, I compared solutions where ChesROMS was forced with only the 10 major rivers from the CBP's watershed model, concentrated forcing versus traditional USGS forcing with only 10 major rivers. These comparisons were made using a standard biogeochemical model parameter set. These comparisons reveal that the diffuse river forcing has potentially large impacts on the simulated water quality of Chesapeake Bay during winter and spring when river flows are large and variable. These effects are most strongly manifested in the tributaries, shorelines, and bottom water in the upper Bay near the Patapsco river. This result contradicts the statement by Feng et al. (2015) that diffuse forcing is likely to have a negligible impact on ChesROMS water quality simulations. However, it is consistent with Ye et al. (2018) who showed that forcing with WSM output can increase the simulation skill for salinity across Chesapeake Bay. Other lab groups working in Chesapeake Bay have utilized this WSM forcing (Testa et al. 2014; Irby et al. 2018) but never in its entirety. For example, Testa et al. (2014) do not use the point source inputs from the CBP WSM. The CBP WSM was designed for regulatory applications and, specifically, for determining nutrient loads under different management scenarios (Shenk, Wu, and Linker 2012).. Because the Chesapeake Bay TMDL is composed of multiple TMDL's for smaller water bodies is it imperative that the numerous tributaries to these smaller water bodies are accounted for. This work suggests that water quality simulations that focus on areas outside the mainstem Bay should utilize WSM forcing.

Diffuse WSM total riverine discharge is very similar to observed USGS discharge for a large portion of the year (Fig. 4a,b). In contrast, the concentrated forcing underestimates the riverine flow into Chesapeake Bay for almost the entire year. As such this method is not employed as a practical forcing method but rather for heuristic purposes. The comparisons presented in this paper reveals that when using the WSM output it is vital to use the entire WSM output, and that using only the 10

largest rivers from the WSM output will significantly underestimate the river flow and nutrient loads.

The divergence of diffuse forcing where discharge becomes larger than that of traditional forcing discharge corresponds to the July 7th (Fig. 4a,b) occurrence of the extratropical cyclone Cindy (Beven et al. 2008). Cindy dropped upwards of seven inches of rain across the state and caused extensive flooding across Maryland. The largest difference between the diffuse and traditional forcing occurs at day 283 which corresponds to a weather event on October 8th in which the remnants of Tropical Storm Tammy and Subtropical Depression 22 combined to cause large flooding in the Northeastern US (Beven et al. 2008). After July, large weather events have increasing influence on the riverine discharge compared to earlier in the year. The diffuse WSM forcing appears to capture these events with greater accuracy than traditional USGS forcing because it includes more diffuse flow from hundreds of small rivers. These differences are likely to be particularly pronounced in wet years, or years with large events caused by tropical storms or hurricanes when diffuse inputs are likely to be relatively large compared to the inputs from the major rivers.

Results indicate that the WSM output has a higher NO₃ load compared to USGS forcing (Table. 3). Moreover, with the diffuse forcing the large additions of NO₃ appear to be occurring along the northwestern shore of the Bay near the Patapsco River (Fig 9a, 10a). where there are no NO₃ inputs in the traditional forcing. This is an area which is home to the City of Baltimore and a largely developed metropolitan area. Adding additional inputs along this shoreline add potentially significant sources of water and nutrients which are neglected with the traditional forcing scheme. It is also apparent the largest differences in bottom water salinity occur along the shoreline and within tributaries (Fig. 9f, 10f.). The importance of this is twofold. First, the spatial differences between diffuse and traditional forcing are manifested differently across the Bay. For example, during April, the Choptank and lower York Rivers exhibit higher salinity under a diffuse scheme (Fig. 9f). These regional differences run counter to results covering the remainder of Chesapeake Bay where salinity is higher. In order to better understand this, there is a need for higher resolution modelling to examine localized impacts. Second, the addition of diffuse flows may

not have as large an impact on the mainstem compared to tributaries and closer to the shore. Thus, when diffuse inputs are added, the mainstem tends to behave similarly under the diffuse, traditional and concentrated forcing schemes.

Increased NO_3 loads fuel higher springtime oxygen levels under diffuse forcing. This finding aligns with the theory of (Kemp et al. 2005) which posits that nutrients delivered during the spring freshet foster primary production in the spring which fuel summer hypoxia. Reduced inputs from a concentrated forcing scheme provide reduced hypoxic volume compared to either a diffuse or traditional forcing schemes. It is likely that the main difference in summer hypoxic volume is a result of increased NO_3 inputs from diffuse forcing during the springtime. That is, under the paradigm of Kemp et al. (2005) high springtime primary production fuels more summertime hypoxia. This is not the case with concentrated forcing where the loads are underestimated. Hypoxia also develops slightly earlier and persists much longer under diffuse forcing with the months of October and November having significant hypoxic volume (Fig. 11.). This is compared to the traditional and concentrated forcing schemes that have no hypoxic volume in October and November. This difference appears to be related to diffuse forcing having higher flows (and loads) in the summer and fall compared to the other forcing methods.

In the future it would prove beneficial to examine the differences between the diffuse forcing and an adjusted concentrated forcing such as that employed by (Irby and Friedrichs 2019) where the diffuse inputs from the WSM were combined and added to 15 major river inputs. This could potentially provide insight into how spatial differences in the flow and nutrient loads impact water quality simulations. Increasing the horizontal spatial resolution of ChesROMS would increase the applicability of ChesROMS to regional studies, i.e., increased resolution, combined with diffuse forcing, should significantly increase the skill of ChesROMS in shallow water tributaries.

An additional area of future research pertains to the method of model tuning. In this study tuning was conducted based on the traditional forcing scheme and these same parameters were used when running the model with diffused and concentrated forcing. This method was chosen to reveal difference that can be attributed solely to

differences in forcing. Future efforts might consider retuning ChesROMS under each forcing scheme, which would likely reduce differences in model results between forcing methods and could potentially lead to different conclusions.

Conclusions 5

Coupled physical-biogeochemical models like ChesROMS are sensitive to the different river forcing methods that have been applied to them. Significant differences in flow rate between traditional forcing (i.e., using only USGS measured flow from the 10 major Chesapeake Bay tributaries) and diffuse forcing (i.e., using watershed model output at 1117 locations around the perimeter of Chesapeake Bay) occur at several times during the year. These differences are the most extreme during the early and late portions of the year when river flows are high and more variable. During the summer months, when the flows are lower and less variable, the differences in flow between the diffuse and traditional forcing are small. During high flow periods in the spring, higher nitrogen loads from diffuse forcing drives increased primary production which ultimately fosters increased hypoxic volume and longer persistence of hypoxic water during summer and fall. During low flow periods in summer diffuse inputs are not able to reach far from shore leading to smaller differences in the dynamics of the mainstem Bay. Although oxygen differences between these forcing schemes are not large, diffuse forcing leads to larger hypoxic volume because the oxygen levels are so low that a small change pushes levels below 2mg/L. Towards the end of the year flow and flow variability again increases and discharge becomes consistently larger with diffuse forcing. Under diffuse forcing the largest differences in simulated water quality tend to occur during these wetter periods with higher flow variability. These differences tend to be particularly large within tributaries, and near shore, especially on the western shore of the middle and upper Bay. During these wetter periods diffuse forcing better captures riverine inputs and leads to significant changes in the model solutions. During the summer months the occurrence of extreme weather events have a large impact on the differences in flow from diffuse forcing compared to traditional forcing. Flow increases due to extreme weather during dry periods are better captured with which leads to

differences in simulated water quality, although these water quality differences tend to lag the events. Based on these results it is apparent that diffuse forcing leads to more accurate water quality simulations especially when there are extreme weather events and in tributaries and along the shallow flanks of the mainstem Bay which, in turn, should foster better links to management activities.

Bibliography

- Beven, John L., Lixion A Avila, Eric S Blake, Daniel P Brown, James L Franklin, Richard D Knabb, Richard J Pasch, Jamie R Rhome, and Stacy R Stewart. 2008. 'Atlantic hurricane season of 2005', *Monthly Weather Review*, 136: 1109-73.
- Bever, Aaron J., Marjorie A. M. Friedrichs, Carl T. Friedrichs, Malcolm E. Scully, and Lyon W. J. Lanerolle. 2013. 'Combining observations and numerical model results to improve estimates of hypoxic volume within the Chesapeake Bay, USA', *Journal of Geophysical Research-Oceans*, 118: 4924-44.
- Boynton, W. R., J. H. Garber, R. Summers, and W. M. Kemp. 1995. 'inputs, Transformations, And Transport Of Nitrogen And Phosphorus In Chesapeake Bay And Selected Tributaries', *Estuaries*, 18: 285-314.
- Bradley, Paul B., Marta P. Sanderson, Marc E. Frischer, Jennifer Brofft, Melissa G. Booth, Lee J. Kerkhof, and Deborah A. Bronk. 2010. 'Inorganic and organic nitrogen uptake by phytoplankton and heterotrophic bacteria in the stratified Mid-Atlantic Bight', *Estuarine Coastal and Shelf Science*, 88: 429-41.
- Brown, C. W., R. R. Hood, W. Long, J. Jacobs, D. L. Ramers, C. Wazniak, J. D. Wiggert, R. Wood, and J. Xu. 2013. 'Ecological forecasting in Chesapeake Bay: Using a mechanistic-empirical modeling approach', *Journal of Marine Systems*, 125: 113-25.
- Cerco, C, and M Noel. 2017. 'The 2017 Chesapeake Bay water quality and sediment transport model', US Army Engineer Waterways Experiment Station, Vicksburg MS. https://www.chesapeakebay.net/documents/2017_WQSTM_Documentation_DRAFT_5-10-17.pdf.
- Da, Fei, Marjorie A. M. Friedrichs, and Pierre St-Laurent. 2018. 'Impacts of Atmospheric Nitrogen Deposition and Coastal Nitrogen Fluxes on Oxygen Concentrations in Chesapeake Bay', *Journal of Geophysical Research-Oceans*, 123: 5004-25.
- Fasham, M. J. R., H. W. Ducklow, and S. M. McKelvie. 1990. 'A Nitrogen-Based Model Of Plankton Dynamics In The Oceanic Mixed Layer', *Journal of Marine Research*, 48: 591-639.

- Feng, Yang, Marjorie A. M. Friedrichs, John Wilkin, Hanqin Tian, Qichun Yang, Eileen E. Hofmann, Jerry D. Wiggert, and Raleigh R. Hood. 2015. 'Chesapeake Bay nitrogen fluxes derived from a land-estuarine ocean biogeochemical modeling system: Model description, evaluation, and nitrogen budgets', *Journal of Geophysical Research-Biogeosciences*, 120: 1666-95.
- Fennel, Katja, John Wilkin, Julia Levin, John Moisan, John O'Reilly, and Dale Haidvogel. 2006. 'Nitrogen cycling in the Middle Atlantic Bight: Results from a three-dimensional model and implications for the North Atlantic nitrogen budget', *Global Biogeochemical Cycles*, 20.
- Hood, R. R., G. Shenk, R. Dixon, W. Ball, J. Bash, C. Cerco, P. Claggett, L. Harris, T.F. Ihde, L. Linker, C. Sherwood, and L. Wainger (2019) Chesapeake Bay Program Modeling in 2025 and Beyond: A Proactive Visioning Workshop. STAC Publication Number 18-007, Edgewater, MD. 55 pages.
- Irby, Isaac D., and Marjorie A. M. Friedrichs. 2019. 'Evaluating Confidence in the Impact of Regulatory Nutrient Reduction on Chesapeake Bay Water Quality', *Estuaries and Coasts*, 42: 16-32.
- Irby, Isaac D., Marjorie A. M. Friedrichs, Fei Da, and Kyle E. Hinson. 2018. 'The competing impacts of climate change and nutrient reductions on dissolved oxygen in Chesapeake Bay', *Biogeosciences*, 15: 2649-68.
- Irby, Isaac D., Marjorie A. M. Friedrichs, Carl T. Friedrichs, Aaron J. Bever, Raleigh R. Hood, Lyon W. J. Lanerolle, Ming Li, Lewis Linker, Malcolm E. Scully, Kevin Sellner, Jian Shen, Jeremy Testa, Hao Wang, Ping Wang, and Meng Xia. 2016. 'Challenges associated with modeling low-oxygen waters in Chesapeake Bay: a multiple model comparison', *Biogeosciences*, 13: 2011-28.
- Kemp, W. M., W. R. Boynton, J. E. Adolf, D. F. Boesch, W. C. Boicourt, G. Brush, J. C. Cornwell, T. R. Fisher, P. M. Glibert, J. D. Hagy, L. W. Harding, E. D. Houde, D. G. Kimmel, W. D. Miller, R. I. E. Newell, M. R. Roman, E. M. Smith, and J. C. Stevenson. 2005. 'Eutrophication of Chesapeake Bay: historical trends and ecological interactions', *Marine Ecology Progress Series*, 303: 1-29.

- Kemp, W. M., J. M. Testa, D. J. Conley, D. Gilbert, and J. D. Hagy. 2009. 'Temporal responses of coastal hypoxia to nutrient loading and physical controls', *Biogeosciences*, 6: 2985-3008.
- Pauly, D., and V. Christensen. 1995. 'Primary Production Required To Sustain Global Fisheries', *Nature*, 374: 255-57.
- Scully, Malcolm E. 2016. 'The contribution of physical processes to inter-annual variations of hypoxia in Chesapeake Bay: A 30-yr modeling study', *Limnology and Oceanography*, 61: 2243-60.
- Shchepetkin, A. F., and J. C. McWilliams. 2005. 'The regional oceanic modeling system (ROMS): a split-explicit, free-surface, topography-following-coordinate oceanic model', *Ocean Modelling*, 9: 347-404.
- Shenk, Gary W., Jing Wu, and Lewis C. Linker. 2012. 'Enhanced HSPF Model Structure for Chesapeake Bay Watershed Simulation', *Journal of Environmental Engineering-Asce*, 138: 949-57.
- Testa, Jeremy M, Yun Li, Younjoo J Lee, Ming Li, Damian C Brady, Dominic M Di Toro, and W Michael Kemp. 2017. 'Modeling Physical and Biogeochemical Controls on Dissolved Oxygen in Chesapeake Bay: Lessons Learned from Simple and Complex Approaches.' in, *Modeling Coastal Hypoxia* (Springer).
- Testa, Jeremy M., and W. Michael Kemp. 2014. 'Spatial and Temporal Patterns of Winter-Spring Oxygen Depletion in Chesapeake Bay Bottom Water', *Estuaries and Coasts*, 37: 1432-48.
- Testa, Jeremy M., Yun Li, Younjoo J. Lee, Ming Li, Damian C. Brady, Dominic M. Di Toro, W. Michael Kemp, and James J. Fitzpatrick. 2014. 'Quantifying the effects of nutrient loading on dissolved O₂ cycling and hypoxia in Chesapeake Bay using a coupled hydrodynamic-biogeochemical model', *Journal of Marine Systems*, 139: 139-58.
- Van Valkenburg, Shirley D., Joanne K. Jones, and Donald R. Heinle. 1978. 'A comparison by size class and volume of detritus versus phytoplankton in Chesapeake Bay', *Estuarine and Coastal Marine Science*, 6: 569-82.
- Wang, Hao. 2019. 'Transport and Fate of Particulate Organic Nitrogen in Chesapeake Bay; A numerical study', *Manuscript in Progress*

- Warner, J. C., W. R. Geyer, and J. A. Lerczak. 2005. 'Numerical modeling of an estuary: A comprehensive skill assessment', *Journal of Geophysical Research-Oceans*, 110.
- Wiggert, Jerry D, Raleigh R Hood, and Christopher W Brown. 2017. 'Modeling hypoxia and its ecological consequences in Chesapeake Bay.' in, *Modeling Coastal Hypoxia* (Springer).
- Williams, Michael R., Solange Filoso, Benjamin J. Longstaff, and William C. Dennison. 2010. 'Long-Term Trends of Water Quality and Biotic Metrics in Chesapeake Bay: 1986 to 2008', *Estuaries and Coasts*, 33: 1279-99.
- Willmott, C. J., S. G. Ackleson, R. E. Davis, J. J. Feddema, K. M. Klink, D. R. Legates, J. Odonnell, and C. M. Rowe. 1985. 'STATISTICS FOR THE EVALUATION AND COMPARISON OF MODELS', *Journal of Geophysical Research-Oceans*, 90: 8995-9005.
- Xu, J. T., R. R. Hood, and S. Y. Chao. 2005. 'A simple empirical optical model for simulating light attenuation variability in a partially mixed estuary', *Estuaries*, 28: 572-80.
- Xu, Jiangtao, and Raleigh R. Hood. 2006. 'Modeling biogeochemical cycles in Chesapeake Bay

Table 1. Model Run Descriptions

Run Name	Forcing Scheme
Diffuse Forcing	1117 freshwater input locations from watershed model
Traditional Forcing	10 major USGS freshwater input locations
Concentrated Forcing	10 major freshwater input locations from watershed model

Table 2. Comparison of annual hypoxic volume for difference forcing schemes.

	Annual Hypoxic Volume (km ³)
Diffuse Forcing	265.05
Traditional Forcing	204.54
Concentrated Forcing	110.54

Table 3. Comparison of summed annual Nitrate Load for the entire Chesapeake Bay, 2005

	Annual NO ₃ Loading (kg/year)
Diffuse Forcing	86,154,632
Traditional Forcing	61,955,984
Concentrated Forcing	64,933,500

Figure 1. a) ChesROMS grid domain; b) Bathymetric plot of ChesROMS model with 10 major rivers from a traditional forcing scheme.

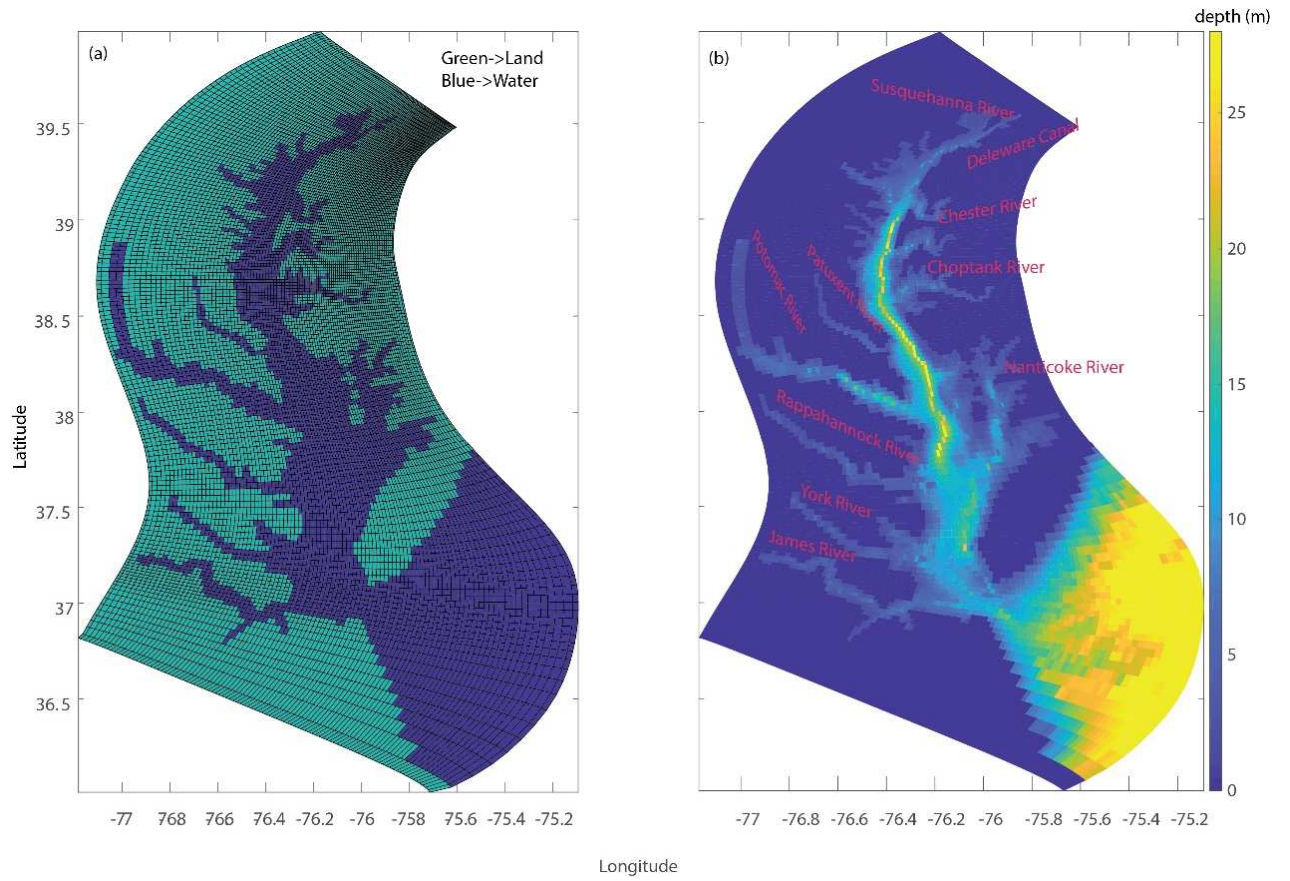


Figure 2. Biogeochemical flows throughout ChesROMS Wiggert et al. (2017)

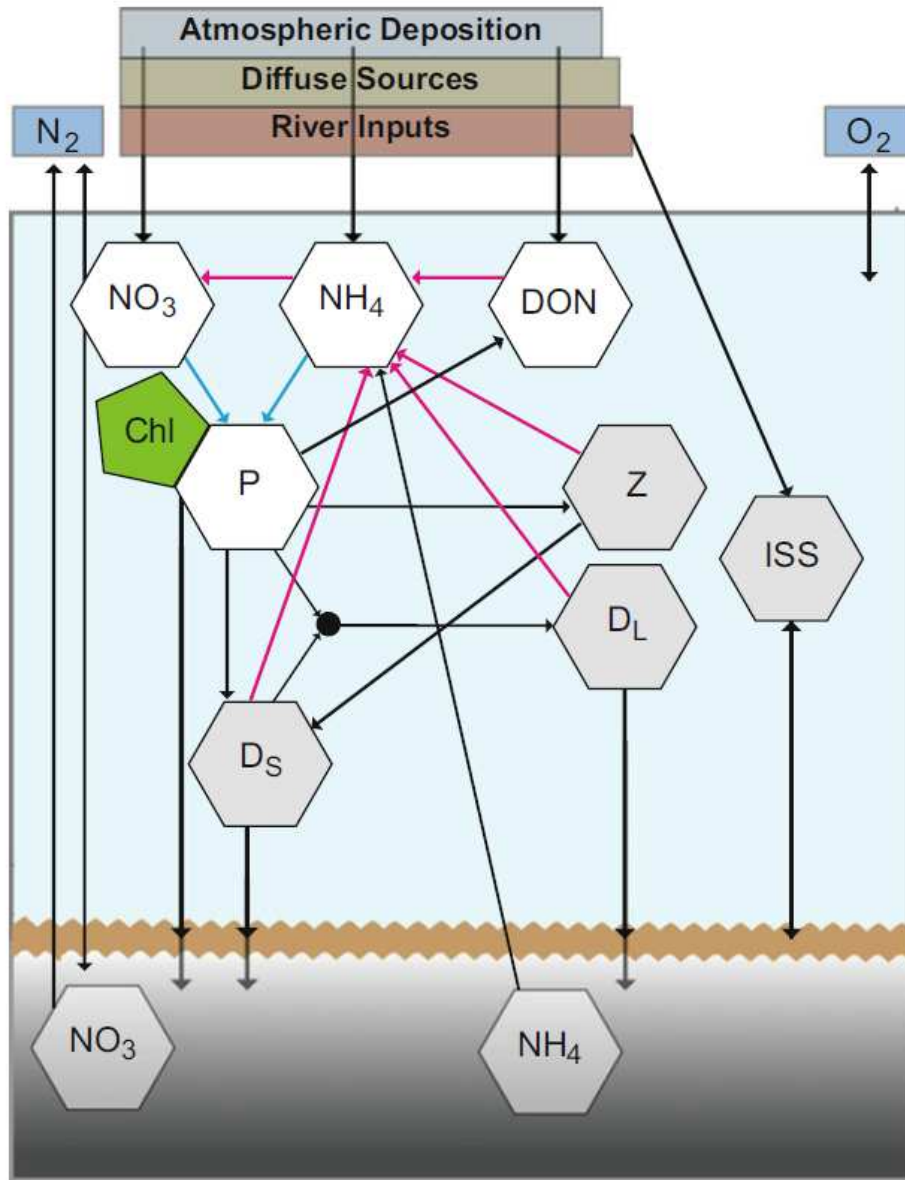


Figure 3. Comparison of Concentrated vs Diffuse River Forcing input locations into Chesapeake Bay.

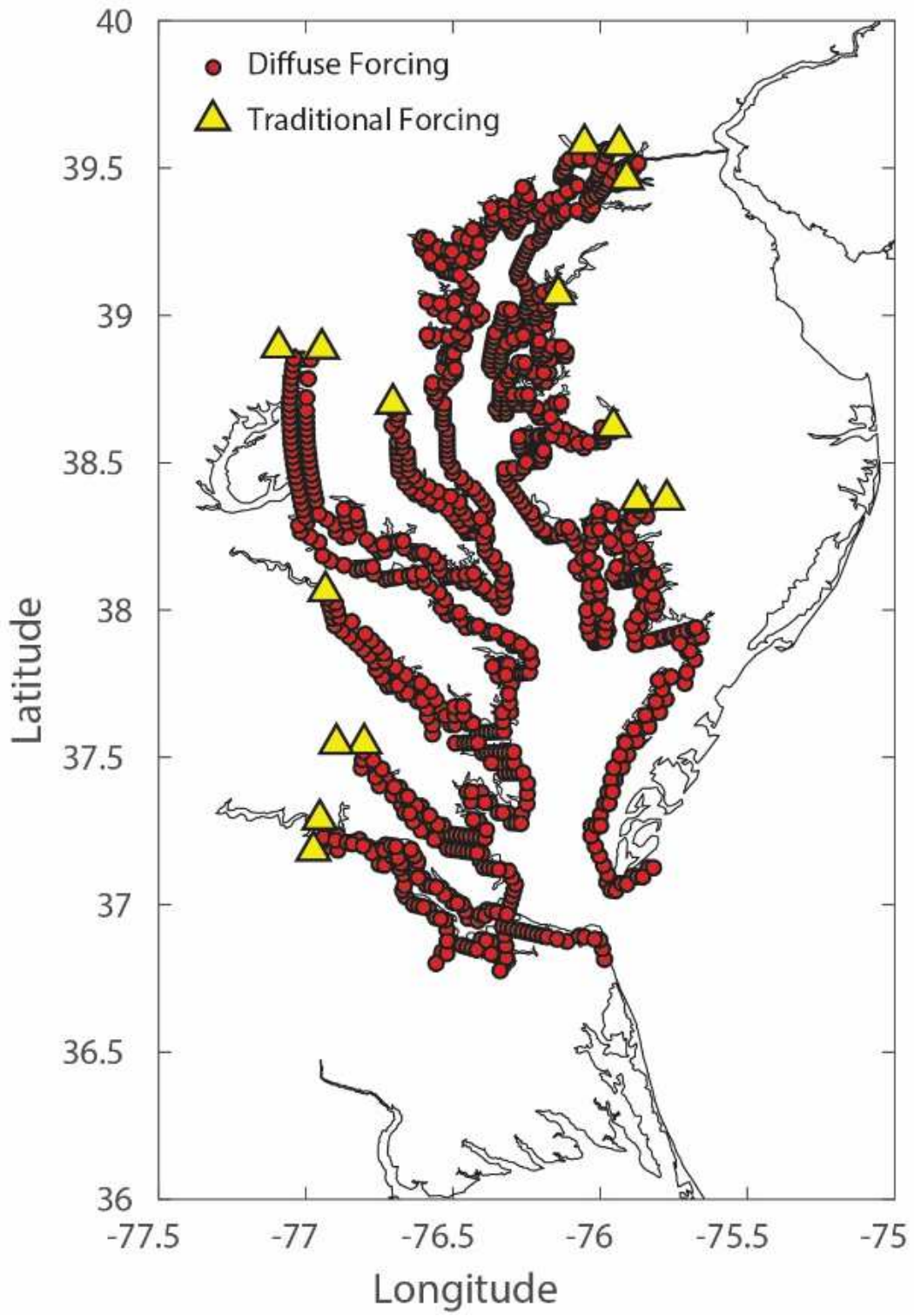


Figure 4. (a) Comparison of the cumulative sum of river discharge for each forcing scheme over the course of 2005 and (b) a comparative time series of total riverine discharge into Chesapeake Bay for 2005.

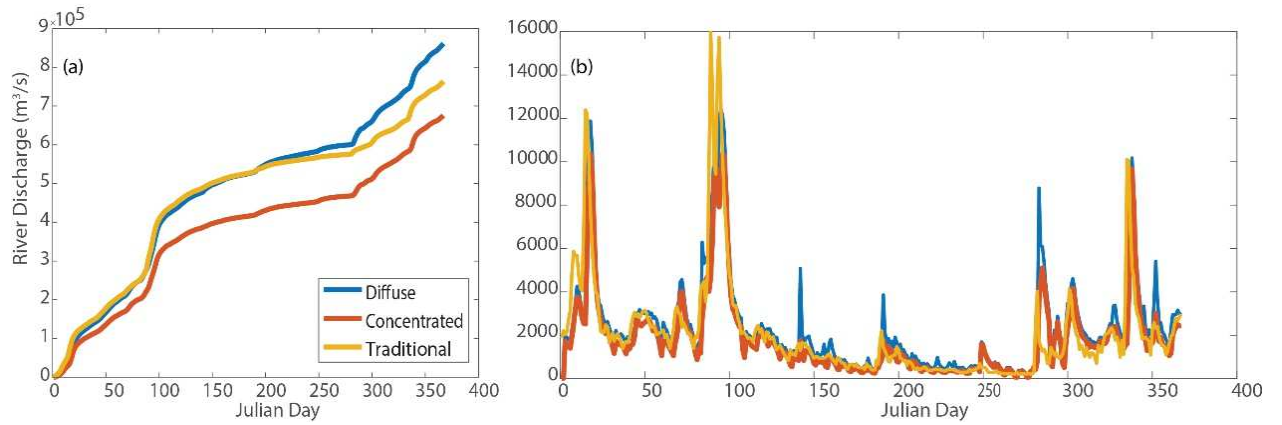


Figure 5. Model skill results from validation of a Traditional forcing scheme plotted spatially for a) Chlorophyll, b) NH₄, c) NO₃, d) Oxygen, e) Salt, f) Temperature.

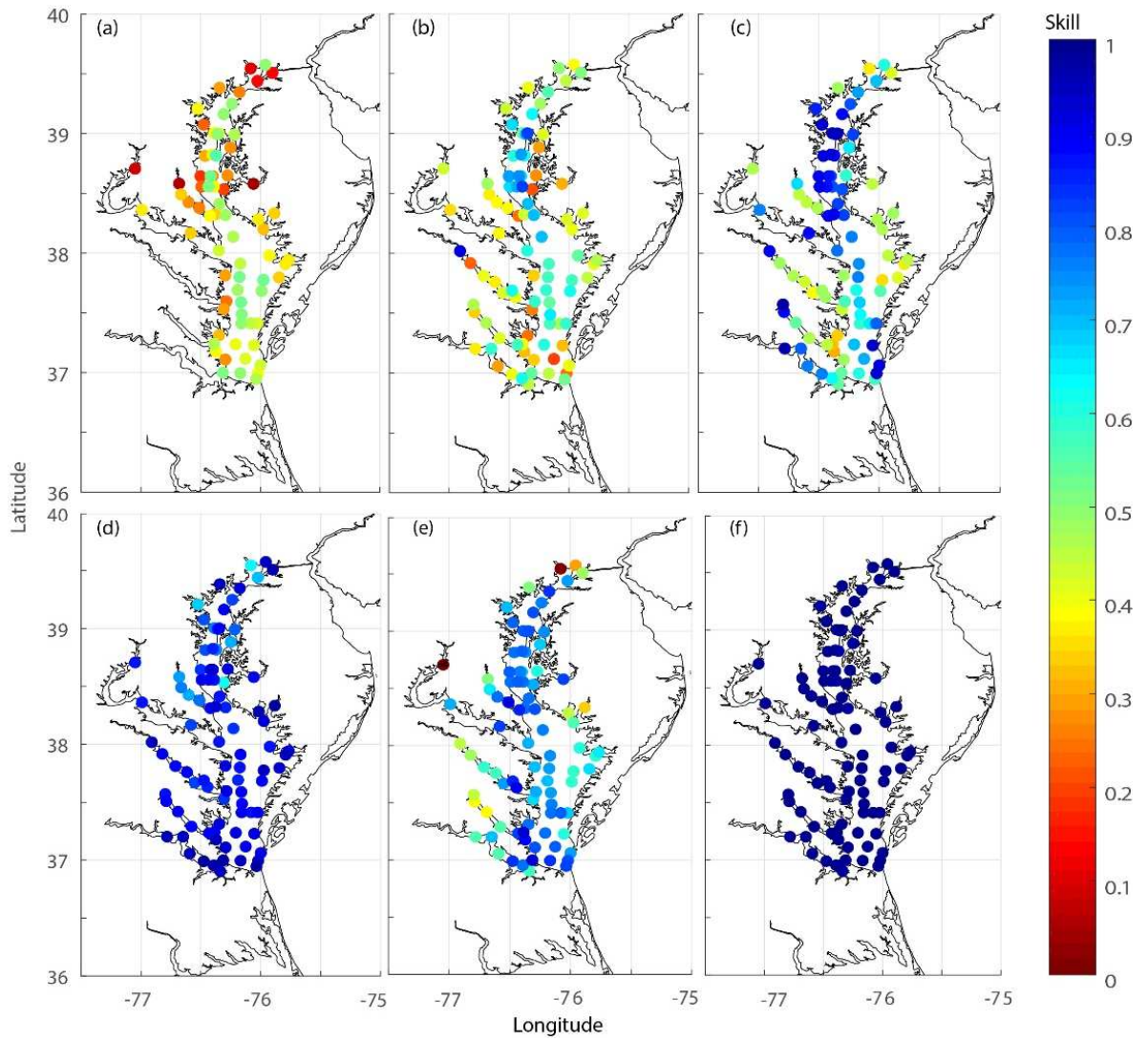


Figure 6. Model skill results from validation of a Diffuse forcing scheme plotted spatially for a) Chlorophyll, b) NH₄, c) NO₃, d) Oxygen, e) Salt, f) Temperature.

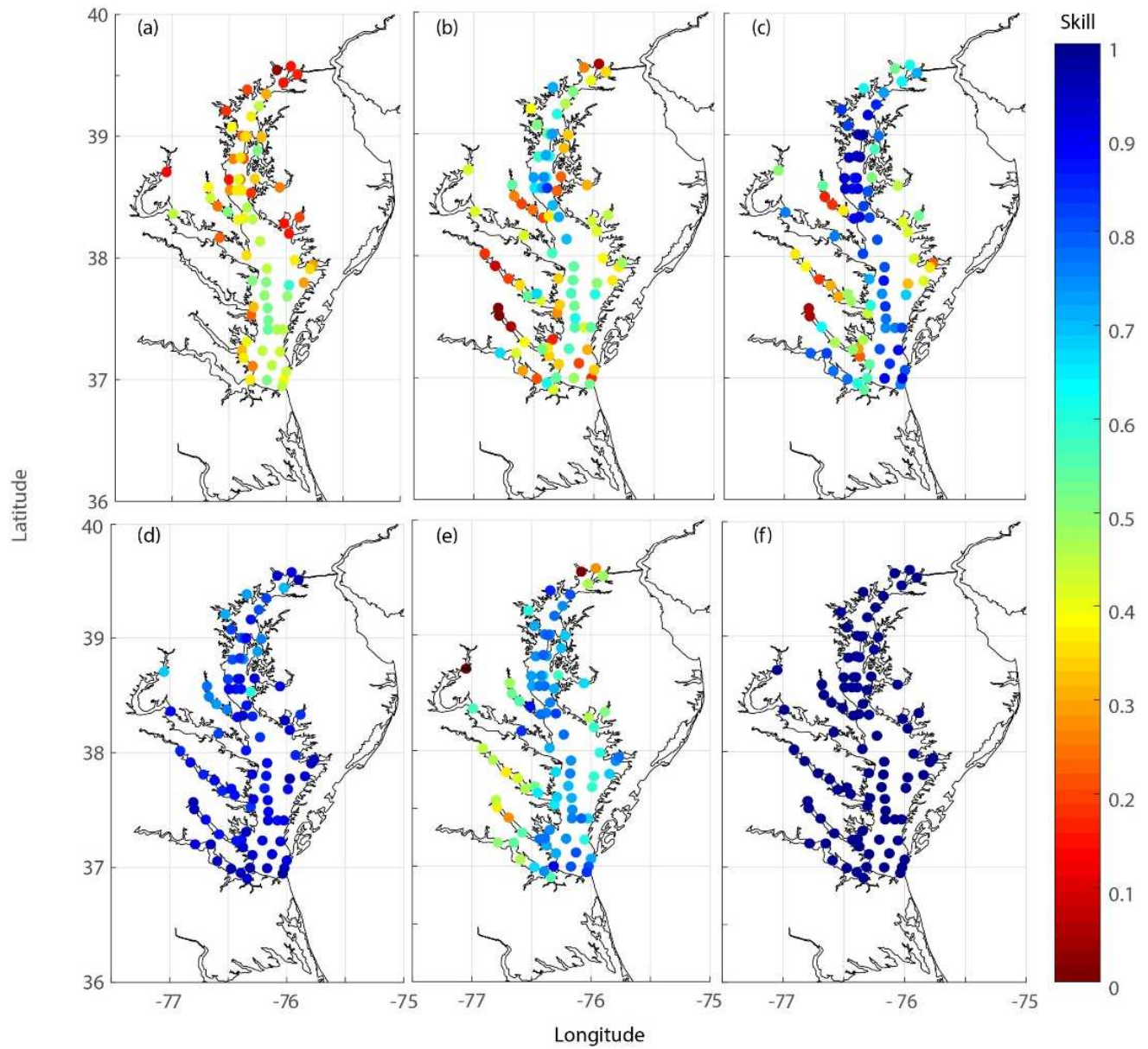


Figure 7. Model skill results from validation of a Concentrated forcing scheme plotted spatially for a)Chlorophyll, b)NH₄, c)NO₃, d)Oxygen, e)Salt, f) Temperature.

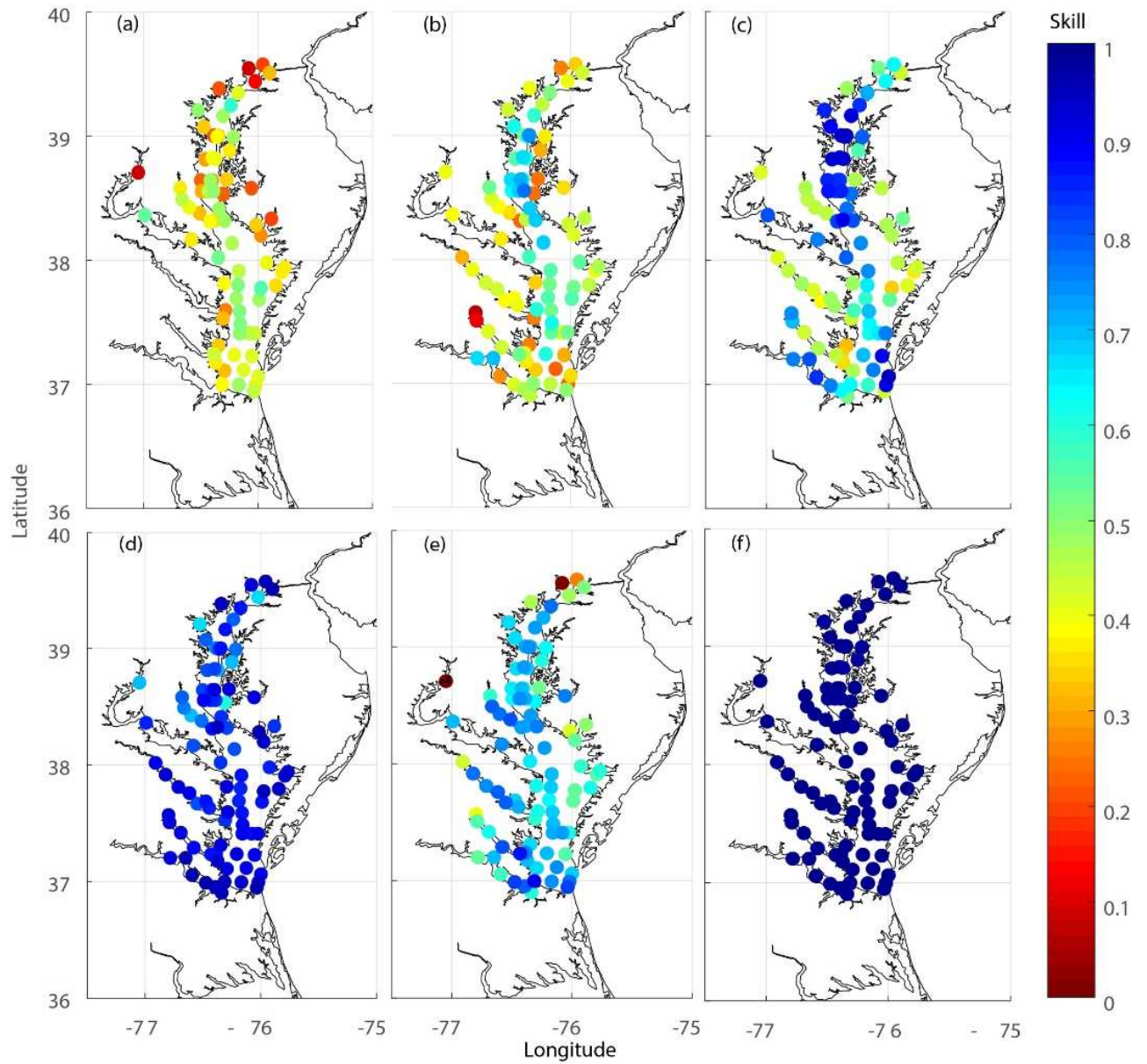


Figure 8. Comparison of monthly averaged difference values for NH₄ (a,f), NO₃ (b,g), oxygen (c,h), salinity (d,i) and temperature (e,j) for the diffuse and concentrated forcing cases compared to traditional forcing for each ChesROMS cell along a vertical section over the entire length of the mainstem Chesapeake Bay deep channel. The differences between diffuse and traditional forcing cases are shown in left hand panels and the differences between the concentrated and traditional forcing cases are shown in the right-hand panels.

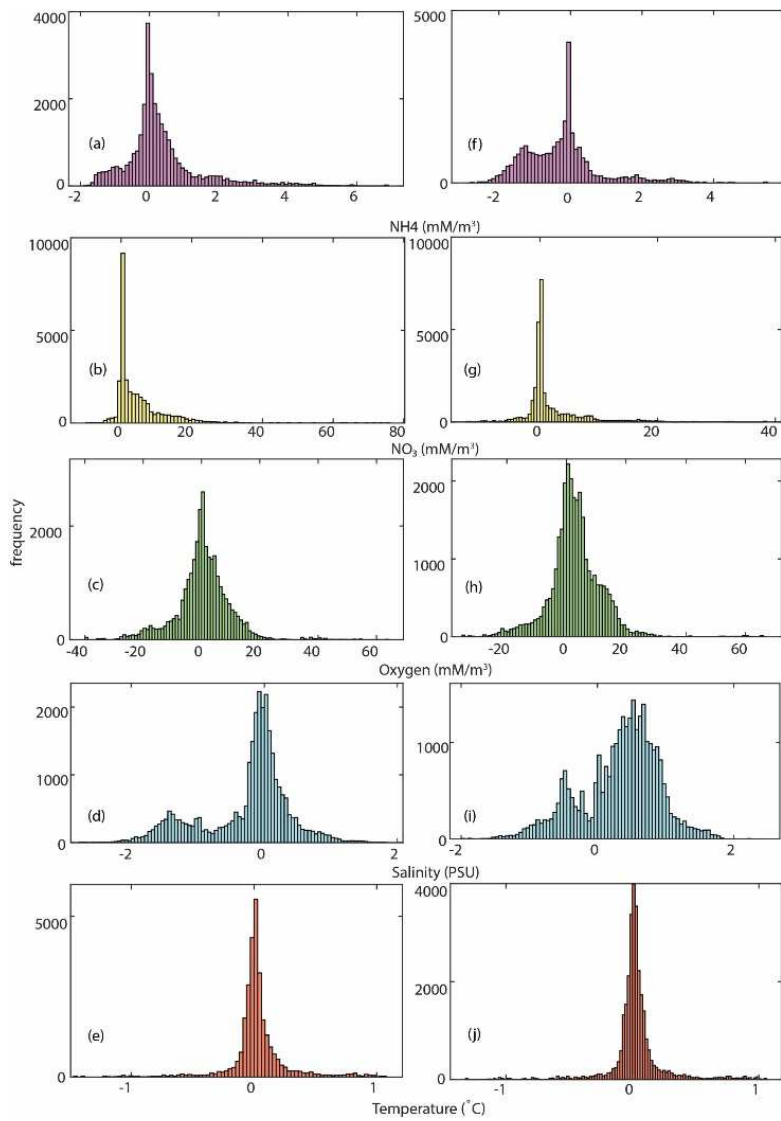


Figure 9. Months of largest differences between Diffuse and Traditional Forcing along a vertical section in the deep channel of the mainstem Bay for a) NO₃, b) Oxygen, c) Salinity, d) Temperature and in the bottom layer of ChesROMS for e) NO₃, f) Oxygen, g) Salinity, h) Temperature.

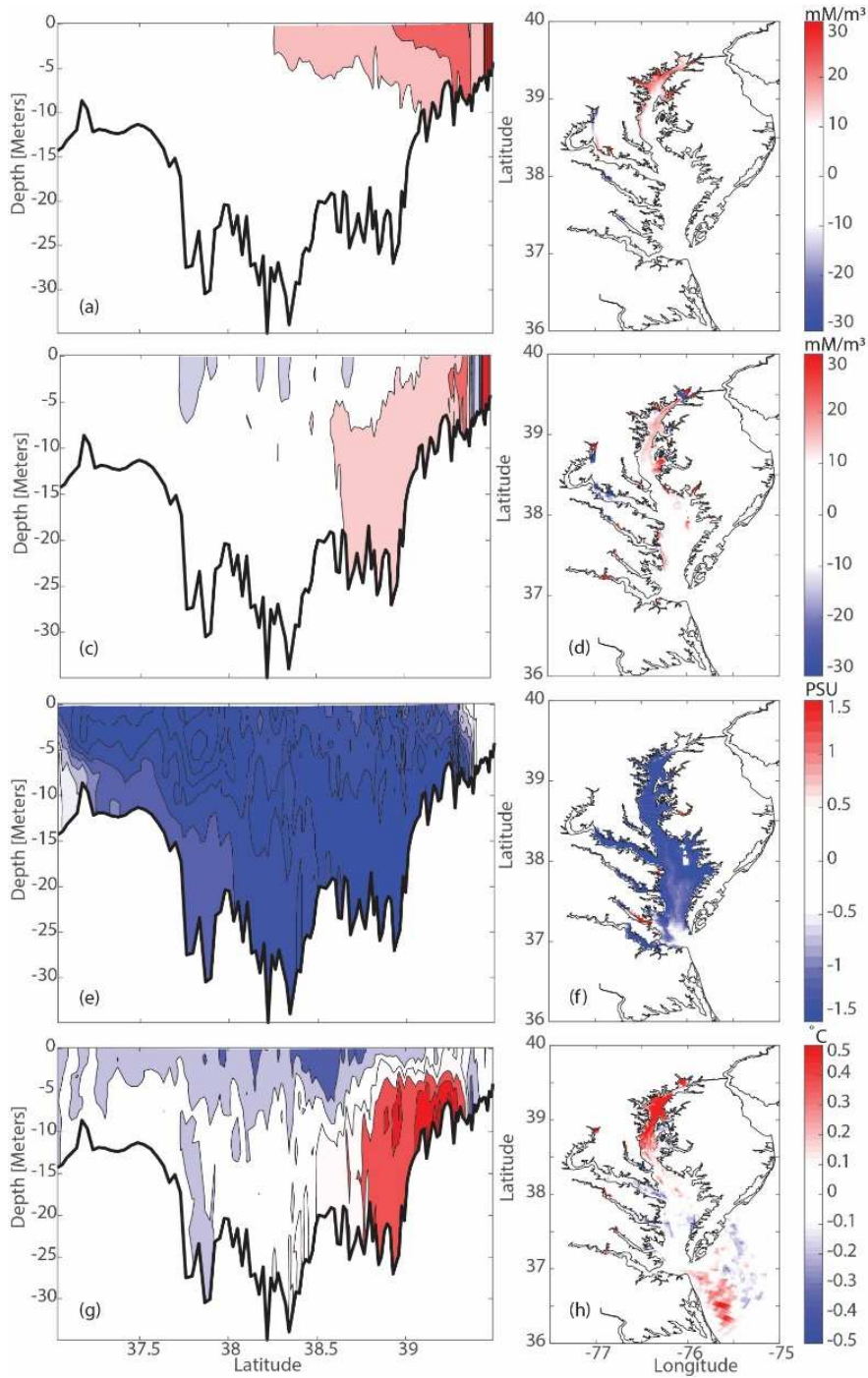


Figure 10. Months of largest differences between Concentrated and Traditional Forcing along a vertical section in the deep channel of the mainstem Bay for a) NO₃, b) Oxygen, c) Salinity, d) Temperature and in the bottom layer of ChesROMS for e) NO₃, f) Oxygen, g) Salinity, h) Temperature.

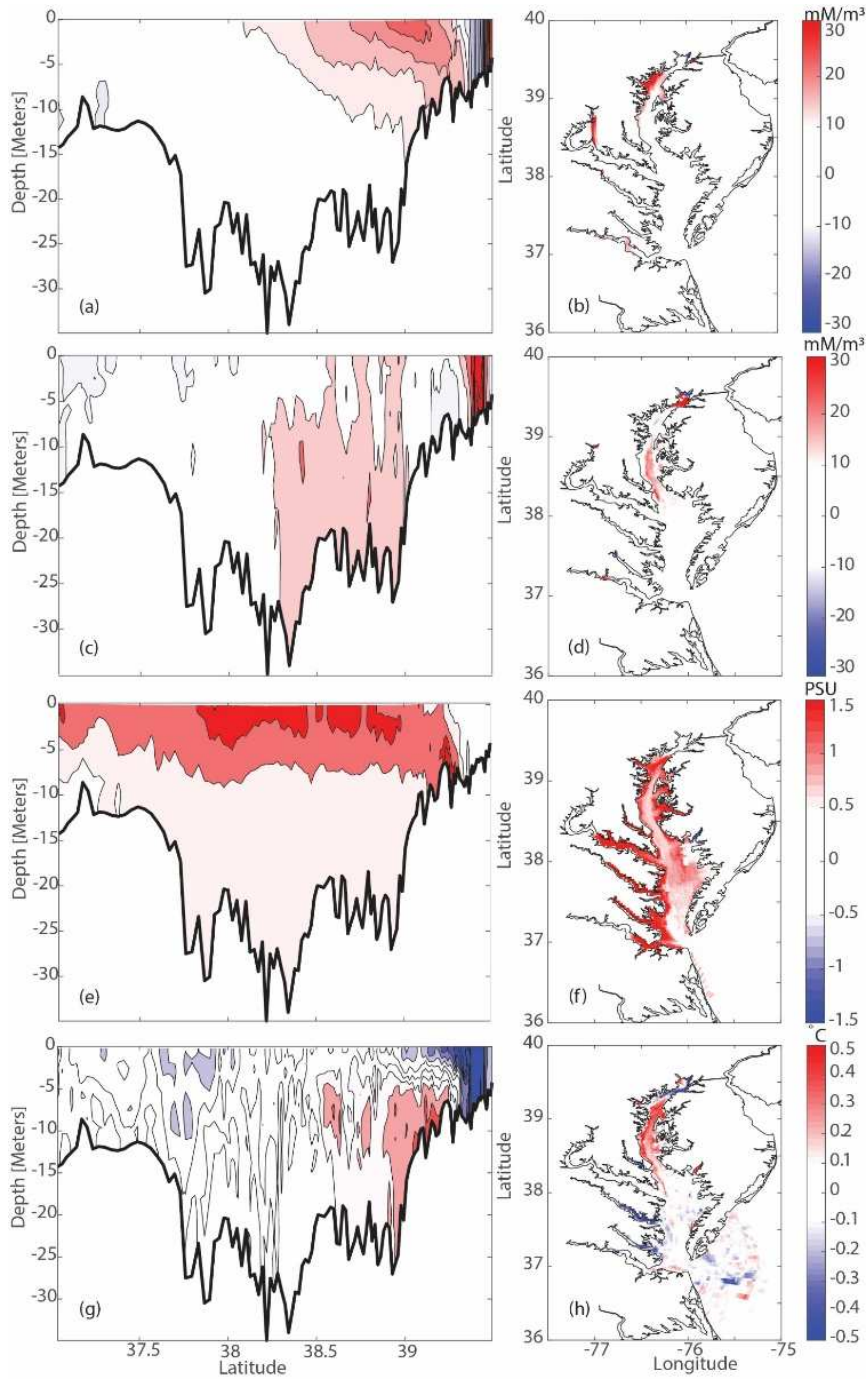


Fig. 11. Averaged monthly hypoxic volume (km³) under different forcing schemes for the year 2005.

